

Supporting Information

Polyplex Exposure Inhibits Cell Cycle, Increases Inflammatory Response, and Can Cause Protein Expression Without Cell Division

Rebecca L. Matz,^{1,2} Blake Erickson,^{2,3} Sriram Vaidyanathan,^{2,5} Jolanta F. Kukowska-Latallo,^{2,4} James R. Baker, Jr.,^{2,4,5} Bradford G. Orr,^{2,6} Mark M. Banaszak Holl*^{1,2,3,5}

¹Department of Chemistry, ²Michigan Nanotechnology Institute for Medicine and Biological Sciences, ³Program in Biophysics, ⁴Department of Internal Medicine, ⁵Department of Biomedical Engineering, ⁶Department of Physics, University of Michigan, Ann Arbor, MI 48109

Experimental

PKH26 Staining – Rationale for Short Incubation Time Prior to Transfection

In order to maximize the dynamic range of the PKH26 fluorescence signal in these experiments, the amount of incubation time prior to transfection was minimized. The cell lines used in these experiments adhered very well to the tissue culture dishes, and throughout the experiments there were no qualitative differences in the adherence of these cell lines as compared to when the seeding times were longer. The control samples (PKH26 only) in Figures 1, 3, S2, and S5 yield a regular doubling time, demonstrating that these seeding times were sufficient to give normal cell division behavior. The data shown in Figure S1, obtained by a method independent of that used in the aforementioned figures, also shows a normal cell doubling time.

Cell Proliferation Assay (Figure S1)

To test whether the proliferation rate of HeLa S3 cells changed upon staining with PKH26, cells were either stained with PKH26 or taken through the staining procedure albeit with no PKH26 present, plated at 80,000 cells/well in 12-well plates with 800 μ L complete medium, and incubated for 5 to 6 h at 37 °C with 5% CO₂ as described. Cells were harvested at various time points over ~2 days for flow cytometry also as previously described with the exception that 7AAD was not employed as a viability stain. The density of the cell suspensions were counted with a BD Accuri C6 Flow Cytometer[®] (Accuri Cytometers; Ann Arbor, MI) which reports the amount of cell suspension volume pulled for a given number of cells, and curves of best exponential fit were again determined using Microsoft[®] Excel[®]. The experiment was repeated three independent times.

pDNA Uptake Assay (Figure S3)

To test the amount of pDNA uptake in HeLa S3 and 293A cells, cells were taken through the PKH26-staining procedure with no PKH26 present, plated at 80,000 cells/well in 12-well plates with 800 μ L complete medium, and incubated for 5 to 6 h at 37 °C with 5% CO₂ as described. Cells were transfected for 3 h as described with polyplexes formed between jetPEITM and blank pDNA labeled with CX-rhodamine (Cat. No. MIR 3125; Mirus Bio; Madison, WI) according to the manufacturer's protocol. After 9 h further incubation in complete medium, the cells were harvested as described and analyzed for CX-rhodamine fluorescence using a BD Accuri C6 Flow Cytometer[®]. See Discussion S1 for full details on data interpretation.

Cellular Senescence Assay (Figure S6)

HeLa S3 and 293A cells were plated in triplicate and transfected as described except that cells were not stained with PKH26 and the experiment was performed in 24-well tissue culture-treated plates (Cat. No. 353047; Becton, Dickinson and Company); all reagents and cell numbers were scaled down according to the growth area of the wells. Following exposure to jetPEITM only or polyplexes formed between jetPEITM and the five types of DNA, cells were tested for cellular senescence (Cat. No. KAA002; EMD Millipore; Billerica, MA) per the manufacturer's instructions at 48 h. The positive control was cells that had been exposed to 50 nM doxorubicin hydrochloride (Cat. No. 2004; AvaChem Scientific; San Antonio, TX) from 3 days prior to transfection through the time point at which cells were assayed for senescence (i.e., for 5 days total). This procedure assesses the activity of senescence-associated β -galactosidase (SA- β -gal) that is identified by blue-green stained cells under light microscopy. Brightfield images were obtained with an Olympus iX70-S1F2 microscope (Olympus Corporation; Tokyo) fitted with an Olympus DP72 digital camera, and the percent of blue-green as compared to normal cells across six separate images for each sample was counted according to previously established protocols.^{1,2}

1. Dimri, G. P.; Lee, X.; Basile, G.; Acosta, M.; Scott, G.; Roskelley, C.; Medrano, E. E.; Linskens, M.; Rubelj, I.; Pereira-Smith, O. A biomarker that identifies senescent human cells in culture and in aging skin in vivo. *Proc. Natl. Acad. Sci. U.S.A.* **1995**, *92*, 9363-9367.

2. Schwarze, S. R.; Fu, V. X.; Desotelle, J. A.; Kenowski, M. L.; Jarrard, D. F. The Identification of Senescence-Specific Genes during Induction of Senescence in Prostate Cancer Cells. *Neoplasia* **2005**, *7*, 816-823.

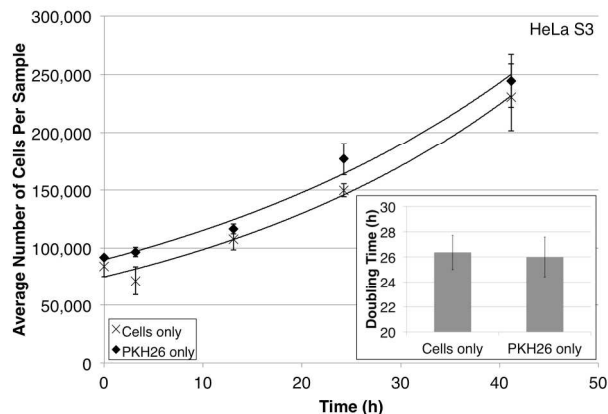


Figure S1. Representative data showing that, as measured by density of cell suspensions, staining with PKH26 does not affect the proliferation rate of HeLa S3 cells as compared to control cells. Each point shows the mean \pm SD of three technical replicates with curve of best exponential fit. The differences in absolute numbers of stained vs unstained cells is likely due to normal variation in cell counting prior to plating. The inset shows summary of data from three independent experiments. $M = 26.0$, $SE = 0.79$ for PKH26-stained cells as compared to $M = 26.4$, $SE = 0.92$ for control cells, $t(4) = 0.30$, $p > 0.05$.

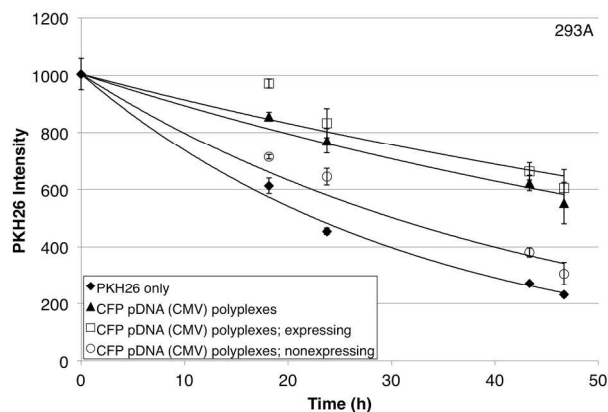


Figure S2. PKH26 intensity of representative 293A cells treated with polyplexes formed between jetPEITM and CFP pDNA over 2 days following transfection as compared to control cells (PKH26 only). Cells expressing CFP (□) and those not expressing CFP (○) are subsets of the whole population (▲) that was treated with polyplexes. Cells were transfected for 3 h beginning at time = 0 h. Each point shows the mean \pm SD of three technical replicates with curve of best exponential fit. All data are fit with PKH26 only data at 0 h.

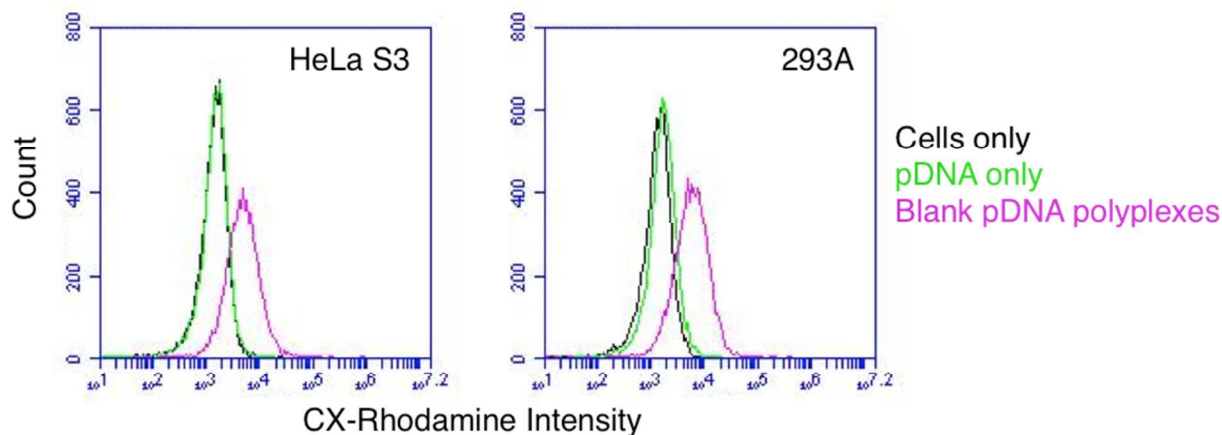


Figure S3. CX-rhodamine fluorescence intensity for representative HeLa S3 and 293A cells treated with polyplexes formed between jetPEITM and CX-rhodamine-labeled blank pDNA. Cells were transfected for 3 h and incubated 9 h further before being harvested and analyzed. For HeLa S3 and 293A cells the entire population of cells exhibits a mean fluorescence shift of 4500 ± 240 and 6200 ± 390 , respectively, consistent with a substantial degree of transfection for all cells in the population. The mean fluorescence shifts are the mean \pm SD of three technical replicates. See Discussion S1 for full details on data interpretation.

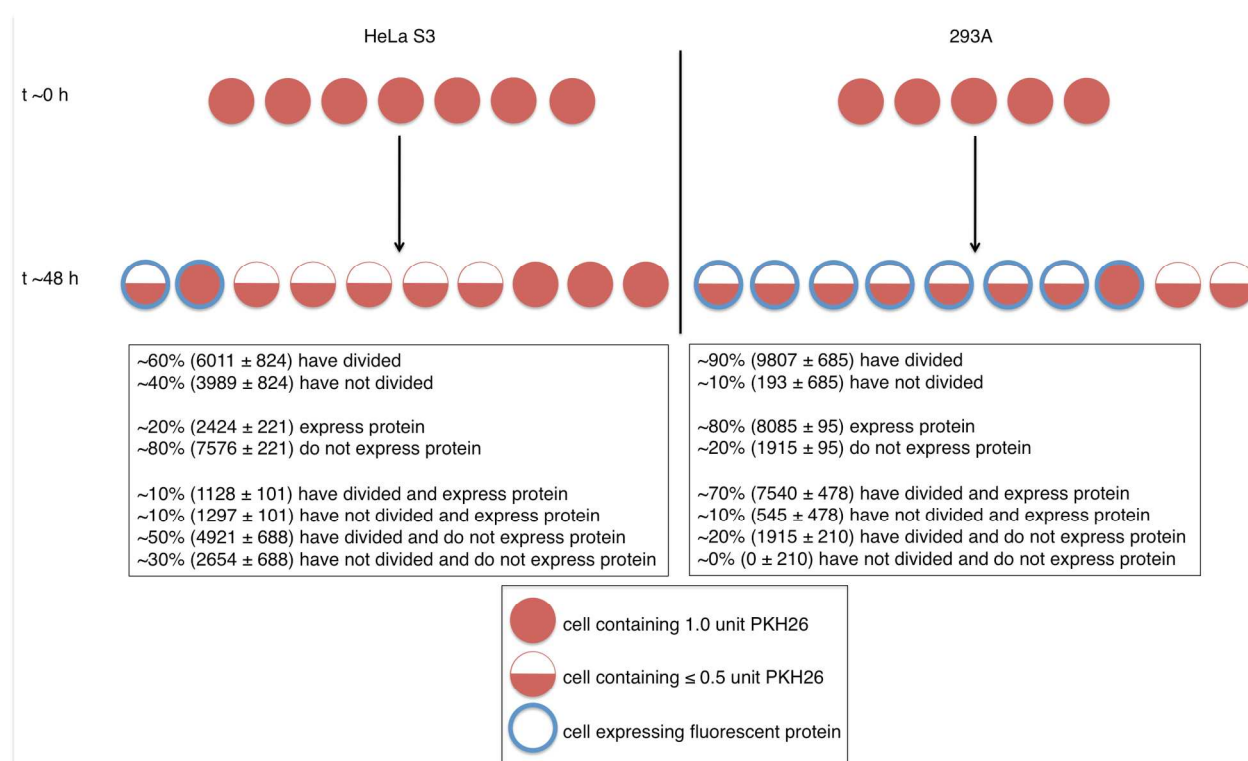


Figure S4. Representative schemes showing the approximate breakdown of divided vs not divided and expressing vs not expressing cells ~48 h following transfection. Division is measured by dilution of the membrane-stable dye PKH26, and expression is measured by fluorescence of the plasmid-encoded protein. The percentages are taken from the data shown in Table 1 (HeLa S3, Expt #1; 293A, Expt #3).

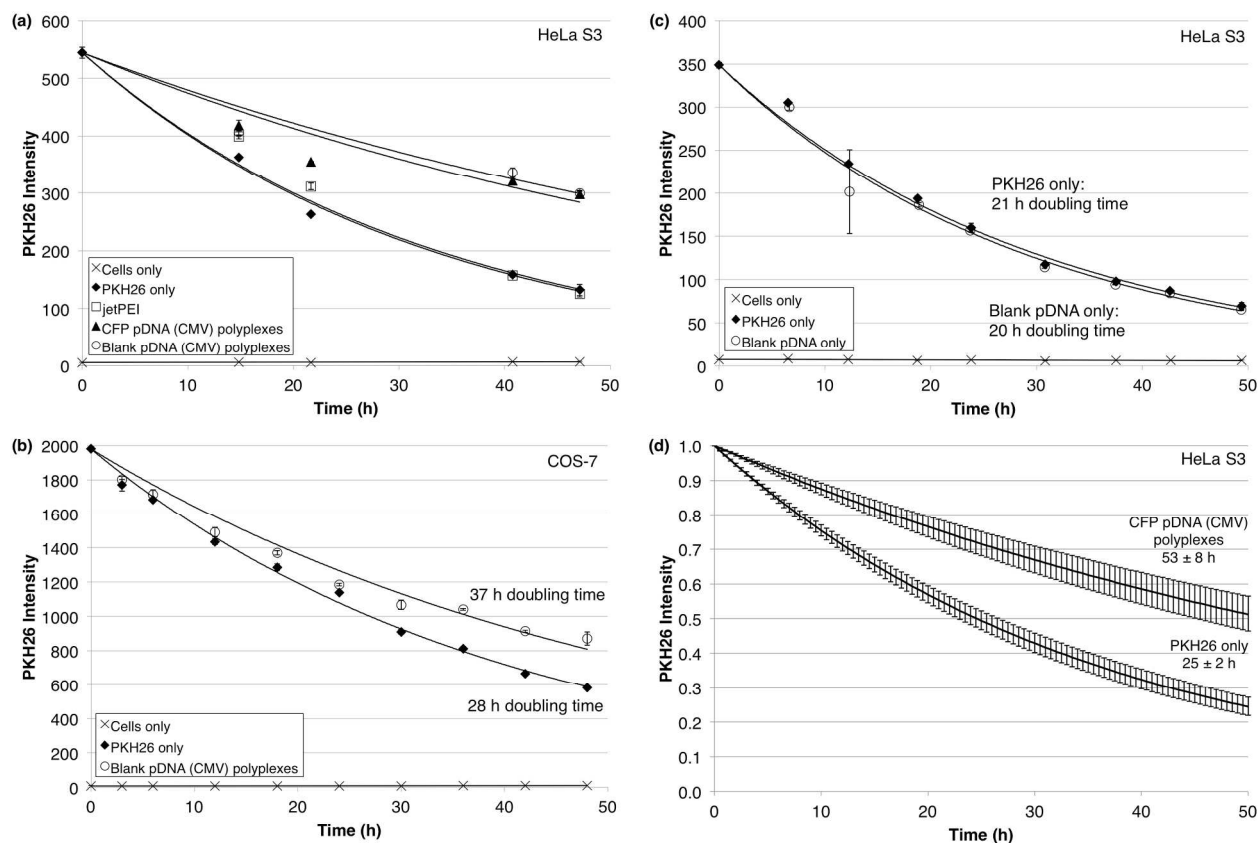


Figure S5. Representative data for (a) HeLa S3 and (b) COS-7 cells showing that exposure to polyplexes slows the doubling time. (c) Representative data for HeLa S3 cells showing that exposure to the pDNA alone did not affect the doubling time. The cells were transfected for 3 h beginning at time = 0 h. Each point shows the mean \pm SD of three technical replicates with curve of best exponential fit except for the cells only sample, which has a linear line of best fit. All data are fit with PKH26 only data at 0 h except for the cells only sample. (d) Average PKH26 intensity of untreated and CFP pDNA (CMV) polyplex-treated HeLa S3 cells over time based on the average doubling times shown in Figure 3b. The standard deviations reflect the standard deviations of the average doubling times.

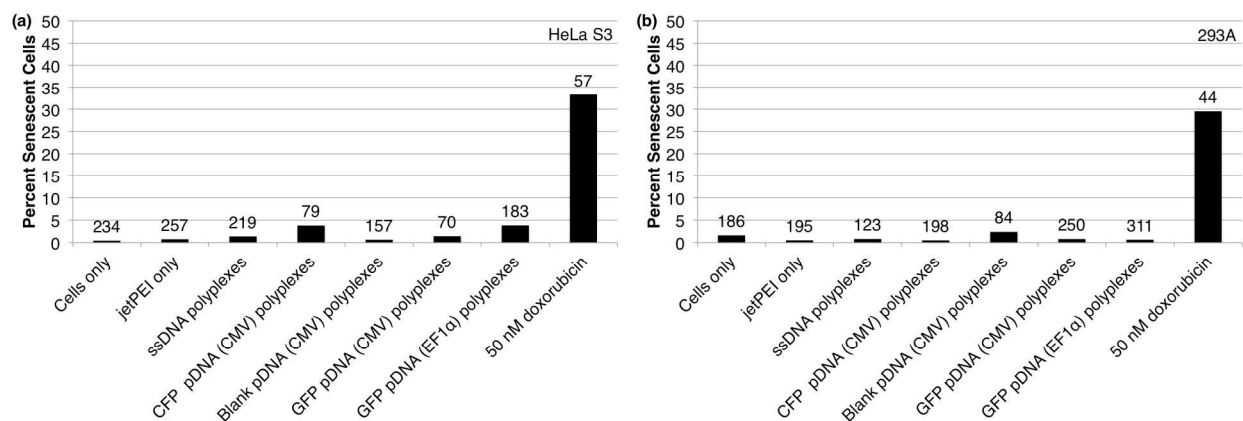
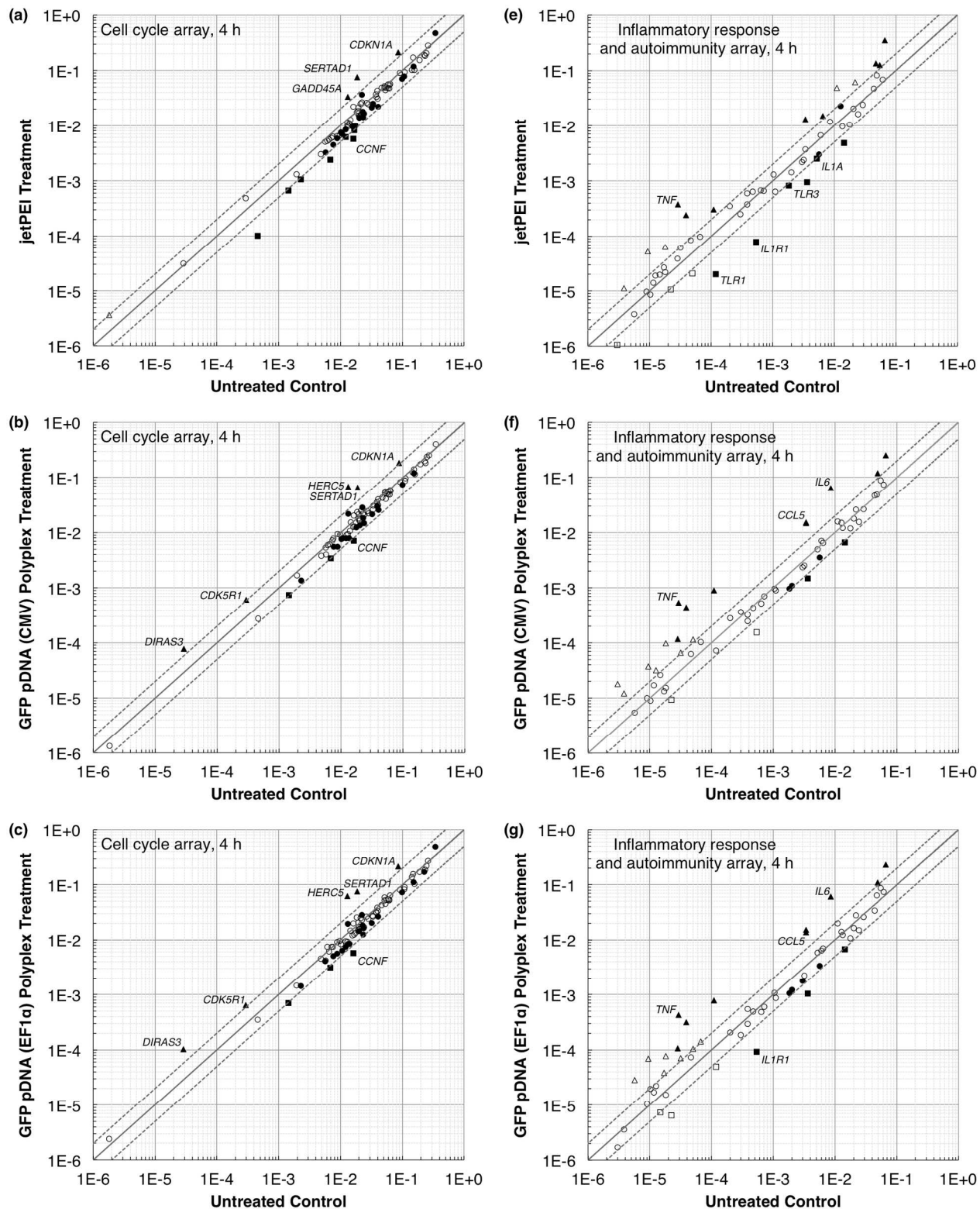


Figure S6. HeLa S3 (a) and 293A (b) cells do not enter cellular senescence upon exposure to the polymer alone (jetPEITM only) or any type of polyplex used in this study. Each data point is labeled with N, the number of cells counted for that sample. N for the doxorubicin case is lower than for the other treatments because there were fewer cells per image due to doxorubicin-induced toxicity. According to Fisher's exact test, no samples are more senescent than the cells only negative control, except for the 50 nM doxorubicin positive control. *** $p < 0.01$.



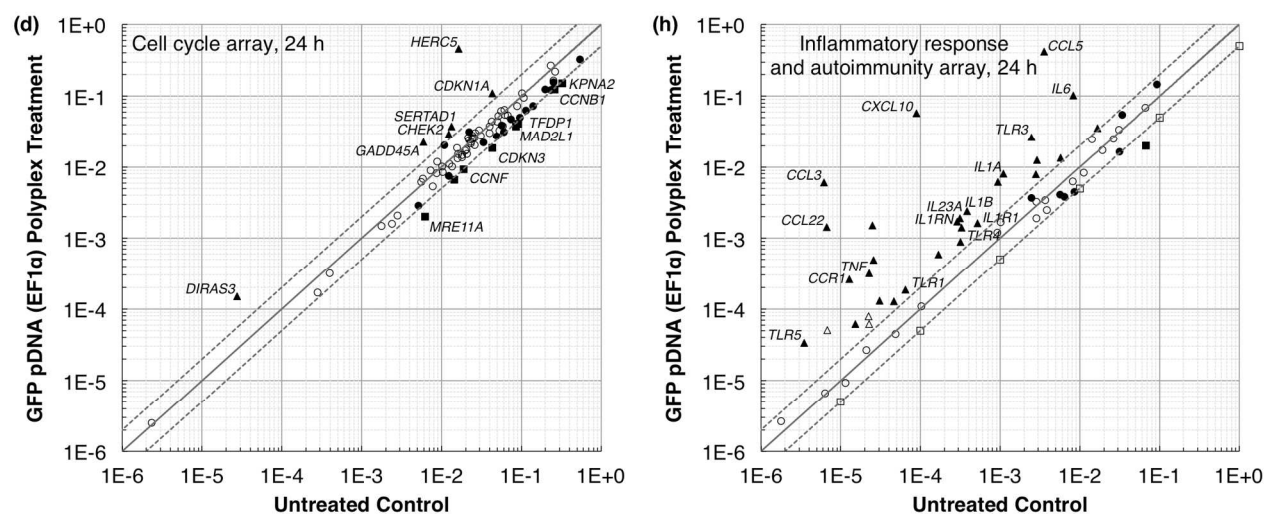


Figure S7. Scatterplots showing the relative number of up- (\blacktriangle) and downregulated (\blacksquare) genes for the jetPEITM, GFP pDNA (CMV) polyplex, and GFP pDNA (EF1 α) polyplex treatments compared to the untreated control at 4 h following transfection. The GFP pDNA (EF1 α) polyplex treatment at 24 h is also shown. (a) – (d) Cell cycle array. (e) – (h) Inflammatory response and autoimmunity array. The centerline indicates a fold change ($2^{-\Delta\Delta C_t}$) of 1, and the upper and lower lines indicate fold changes of 2 in gene expression. Circles indicate fold changes ≤ 2 . Comparing to the untreated control, filled symbols indicate regulation that is significantly different ($p \leq 0.05$), and open symbols indicate regulation that is not significantly different. Only the significantly up- or downregulated genes shown in Tables 2 and 3 are labeled in this figure. Note that the cell cycle array data for the 24 h treatment with GFP pDNA (EF1 α) polyplexes is based on only two biological replicates; the third had to be removed due to evident inhibition of the reverse transcription step.

Table S1. Average doubling times of HeLa S3 and 293A cells exposed to jetPEITM only, or polyplexes made between jetPEITM and ssDNA or various pDNAs.

Treatment	Average Doubling Time (h) ^a	
	HeLa S3	293A
PKH26 only (neg. control)	25 ± 2	25 ± 3
jetPEI TM only	29 ± 2	24 ± 4
ssDNA polyplexes	31 ± 1 **	52 ± 9 **
CFP pDNA (CMV) polyplexes	53 ± 8 ***	46 ± 9 **
Blank pDNA (CMV) polyplexes	52 ± 9 **	35 ± 4 ***
GFP pDNA (CMV) polyplexes	49 ± 8	61 ± 10 *
GFP pDNA (EF1α) polyplexes	52 ± 10	45 ± 16

^a * $p < 0.10$, ** $p < 0.05$, *** $p < 0.01$.

Table S2. Changes in expression of all genes related to the cell cycle pathway in jetPEI™ or polyplex-exposed HeLa S3 cells.

GeneBank	Symbol	Description ^a	Fold Change in Gene Expression ^b					
			jetPEI™		GFP (CMV) polyplexes		GFP (EF1 α) polyplexes	
			4h	24h	4h	24h	4h	24h
NM_005157	ABL1	C-abl oncogene 1, receptor tyrosine kinase	-1.4	1.2	-1.2	1.1	-1.3	1.2
NM_013366	ANAPC2	Anaphase promoting complex subunit 2	-1.6	-1.0	-1.3	-1.2	-1.3	-1.2
NM_013367	ANAPC4	Anaphase promoting complex subunit 4	-1.5	1.1	-1.3	-1.1	-1.7	-1.1
NM_000051	ATM	Ataxia telangiectasia mutated	-2.1	-1.3	-1.7	-1.4	-1.6	-1.4
NM_001184	ATR	Ataxia telangiectasia and Rad3 related	-1.7	-1.1	-1.4	-1.3	-1.5	-1.2
NM_004324	BAX	BCL2-associated X protein	-1.2	1.2	-1.3	-1.1	-1.2	1.1
NM_016567	BCCIP	BRCA2 and CDKN1A interacting protein	-1.2	1.3	-1.1	-1.9	-1.2	-1.9
NM_000633	BCL2	B-cell CLL/lymphoma 2	-1.5	-1.1	-1.2	-1.3	-1.3	-1.5
NM_001168	BIRC5	Baculoviral IAP repeat-containing 5	-1.1	1.0	-1.1	-1.6	-1.4	-1.8
NM_007294	BRCA1	Breast cancer 1, early onset	-1.7	1.3	-1.6	1.1	-1.9	1.2
NM_000059	BRCA2	Breast cancer 2, early onset	-2.9	-1.3	-2.0	1.3	-2.2	1.2
NM_031966	CCNB1	Cyclin B1	-1.3	-1.1	-1.3	-2.1	-1.2	-2.1
NM_004701	CCNB2	Cyclin B2	-1.4	-1.1	-1.3	-1.9	-1.4	-1.8
NM_005190	CCNC	Cyclin C	-1.1	1.1	-1.1	-1.1	-1.1	1.0
NM_053056	CCND1	Cyclin D1	-1.1	1.6	1.3	1.0	1.4	1.1
NM_001759	CCND2	Cyclin D2	2.0	-1.1	-1.4	1.4	1.3	1.1
NM_001238	CCNE1	Cyclin E1	1.4	1.0	1.3	-1.7	1.2	-1.3
NM_001761	CCNF	Cyclin F	-2.8	-1.1	-2.3	-2.0	-2.8	-2.0
NM_004060	CCNG1	Cyclin G1	-1.0	-1.4	-1.1	-1.6	-1.2	-1.4
NM_004354	CCNG2	Cyclin G2	-1.4	-1.4	-1.3	1.0	-1.2	1.2
NM_001239	CCNH	Cyclin H	-1.0	1.0	-1.1	-1.6	-1.0	-1.5
NM_001240	CCNT1	Cyclin T1	1.2	1.5	-1.0	1.1	1.0	1.1
NM_001241	CCNT2	Cyclin T2	-1.2	1.0	-1.0	1.1	1.2	1.1
NM_003903	CDC16	Cell division cycle 16 homolog (S. cerevisiae)	-1.5	1.1	-1.5	-1.1	-1.6	-1.1
NM_001786	CDC2	Cell division cycle 2, G1 to S and G2 to M	-1.4	-1.1	-1.2	-1.9	-1.3	-1.9
NM_001255	CDC20	Cell division cycle 20 homolog (S. cerevisiae)	-1.2	-1.0	-1.1	-1.6	-1.1	-1.6
NM_004359	CDC34	Cell division cycle 34 homolog (S. cerevisiae)	-1.0	1.2	-1.1	1.0	-1.3	1.2
NM_001798	CDK2	Cyclin-dependent kinase 2	1.0	-1.1	1.0	-1.3	1.0	-1.1
NM_000075	CDK4	Cyclin-dependent kinase 4	-1.3	-1.0	-1.2	-1.8	-1.3	-1.9
NM_003885	CDK5R1	Cyclin-dependent kinase 5, regulatory subunit 1 (p35)	1.6	-1.1	2.0	-2.2	2.2	-1.6
NM_016408	CDK5RAP1	CDK5 regulatory subunit associated protein 1	-1.2	-1.1	-1.1	-1.1	-1.1	-1.1
NM_001259	CDK6	Cyclin-dependent kinase 6	-1.1	1.2	1.1	-1.9	1.1	-1.8
NM_001799	CDK7	Cyclin-dependent kinase 7	1.2	1.1	1.2	1.1	1.2	1.1
NM_001260	CDK8	Cyclin-dependent kinase 8	-1.8	1.2	-1.4	-1.4	-1.3	-1.4
NM_000389	CDKN1A	Cyclin-dependent kinase inhibitor 1A (p21, Cip1)	2.5	1.4	2.2	2.1	2.5	2.6
NM_004064	CDKN1B	Cyclin-dependent kinase inhibitor 1B (p27, Kip1)	-1.4	1.1	-1.6	-1.3	-1.5	-1.2
NM_000077	CDKN2A	Cyclin-dependent kinase inhibitor 2A (melanoma, p16, inhibits CDK4)	-1.0	1.0	-1.1	1.0	-1.1	1.1
NM_004936	CDKN2B	Cyclin-dependent kinase inhibitor 2B (p15, inhibits CDK4)	1.7	1.2	1.3	-1.0	1.3	1.0
NM_005192	CDKN3	Cyclin-dependent kinase inhibitor 3	-1.3	-1.1	-1.3	-2.3	-1.2	-2.3
NM_001274	CHEK1	CHK1 checkpoint homolog (S. pombe)	-1.3	1.0	-1.3	-1.1	-1.3	1.1
NM_007194	CHEK2	CHK2 checkpoint homolog (S. pombe)	-1.2	-1.3	1.0	2.2	1.0	2.4
NM_001826	CKS1B	CDC28 protein kinase regulatory subunit 1B	1.1	1.2	-1.0	1.2	1.0	1.2
NM_001827	CKS2	CDC28 protein kinase regulatory subunit 2	1.4	-1.2	1.2	-1.8	1.4	-1.7
NM_003592	CUL1	Cullin 1	-1.3	1.1	-1.1	-1.4	-1.3	-1.3
NM_003591	CUL2	Cullin 2	-1.3	-1.0	-1.2	-1.4	-1.4	-1.3
NM_003590	CUL3	Cullin 3	-4.5	-1.4	-1.7	-1.1	-1.3	-1.3
NM_004399	DDX11	DEAD/H (Asp-Glu-Ala-Asp/His) box polypeptide 11 (CHL1-like helicase homolog, S. cerevisiae)	-1.4	1.1	-1.2	-1.1	-1.2	-1.1
NM_004675	DIRAS3	DIRAS family, GTP-binding RAS-like 3	1.1	-2.8	2.7	4.2	3.5	5.5
NM_004945	DNM2	Dynamain 2	-1.5	1.3	-1.1	1.3	-1.0	1.3
NM_001950	E2F4	E2F transcription factor 4, p107/p130-binding	-1.3	1.1	-1.3	-1.1	-1.7	-1.2
NM_001924	GADD45A	Growth arrest and DNA-damage-inducible, alpha	2.5	4.0	1.6	3.6	1.5	3.8
NM_005316	GTF2H1	General transcription factor IIIH, polypeptide 1, 62kDa	-1.1	1.2	1.1	1.0	1.0	-1.0

NM_016426	GTSE1	G-2 and S-phase expressed 1	-1.3	-1.4	-1.4	-2.*	-1.4	-1.6
NM_016323	HERC5	Hect domain and RLD 5	-1.1	1.4	5.3	25.8	4.8	27.9
NM_004507	HUS1	HUS1 checkpoint homolog (S. pombe)	-1.4	-1.0	-1.5	-1.5	-1.3	-1.4
NM_014708	KNTC1	Kinetochore associated 1	-1.4	-1.1	-1.4	-1.1	-1.3	-1.1
NM_002266	KPNA2	Karyopherin alpha 2 (RAG cohort 1, importin alpha 1)	-1.2	-1.5	-1.0	-2.3	-1.1	-2.1
NM_002358	MAD2L1	MAD2 mitotic arrest deficient-like 1 (yeast)	-1.1	-1.2	-1.1	-2.2	1.0	-2.3
NM_006341	MAD2L2	MAD2 mitotic arrest deficient-like 2 (yeast)	-1.3	-1.2	-1.3	-1.5	-1.2	-1.6
NM_004526	MCM2	Minichromosome maintenance complex component 2	-1.1	1.2	-1.1	-1.2	-1.1	-1.1
NM_002388	MCM3	Minichromosome maintenance complex component 3	-1.2	-1.2	-1.1	-1.3	-1.3	-1.2
NM_005914	MCM4	Minichromosome maintenance complex component 4	-1.2	-1.1	-1.2	-1.2	-1.1	-1.1
NM_006739	MCM5	Minichromosome maintenance complex component 5	1.1	-1.2	-1.1	-1.4	-1.1	-1.2
NM_002417	MKI67	Antigen identified by monoclonal antibody Ki-67	-1.5	1.3	-1.3	-1.1	-1.5	-1.2
NM_002431	MNAT1	Menage a trois homolog 1, cyclin H assembly factor (Xenopus laevis)	1.1	1.2	1.1	1.3	1.1	1.4
NM_005590	MRE11A	MRE11 meiotic recombination 11 homolog A (S. cerevisiae)	-1.6	-1.5	-1.3	-2.6	-1.1	-3.1
NM_002485	NBN	Nibrin	-2.0	-1.4	-1.5	-1.2	-1.6	-1.2
NM_182649	PCNA	Proliferating cell nuclear antigen	1.1	-1.3	-1.1	-1.7	1.0	-1.6
NM_002853	RAD1	RAD1 homolog (S. pombe)	-1.4	-1.3	-1.7	-1.9	-1.6	-2.2
NM_002873	RAD17	RAD17 homolog (S. pombe)	-1.5	-1.0	-1.6	-1.3	-1.6	-1.3
NM_002875	RAD51	RAD51 homolog (RecA homolog, E. coli) (S. cerevisiae)	-2.2	-1.1	-2.0	-1.2	-2.1	-1.2
NM_004584	RAD9A	RAD9 homolog A (S. pombe)	-1.2	1.1	1.0	1.9	1.0	1.9
NM_000321	RB1	Retinoblastoma 1	-1.4	-1.0	-1.3	-1.1	-1.2	-1.0
NM_002894	RBBP8	Retinoblastoma binding protein 8	1.1	-1.0	1.0	-1.0	-1.0	1.0
NM_002895	RBL1	Retinoblastoma-like 1 (p107)	-1.4	1.2	-1.1	1.0	-1.4	1.0
NM_005611	RBL2	Retinoblastoma-like 2 (p130)	-1.8	-1.3	-1.4	1.2	-1.3	1.1
NM_002947	RPA3	Replication protein A3, 14kDa	-1.1	-1.3	-1.1	1.1	-1.0	1.1
NM_013376	SERTAD1	SERTA domain containing 1	4.1	1.7	3.5	2.8	4.1	2.8
NM_005983	SKP2	S-phase kinase-associated protein 2 (p45)	-1.8	-1.3	-1.6	-1.9	-1.5	-1.9
NM_003352	SUMO1	SMT3 suppressor of mif two 3 homolog 1 (S. cerevisiae)	-1.2	-1.8	-1.3	-1.6	-1.2	-1.5
NM_007111	TFDP1	Transcription factor Dp-1	-1.2	-1.2	-1.3	-2.1	-1.2	-2.2
NM_006286	TFDP2	Transcription factor Dp-2 (E2F dimerization partner 2)	-1.4	-1.1	1.1	-1.0	1.0	-1.0
NM_000546	TP53	Tumor protein p53	-2.0	-1.7	-1.3	-1.6	-1.3	-1.6
NM_003334	UBA1	Ubiquitin-like modifier activating enzyme 1	-1.4	-1.3	-1.1	-1.5	-1.0	-1.5

^aThe gene descriptions are reproduced from the array product information from Qiagen. ^bGreen and red shading indicate fold-changes of ≥ 2 and ≤ -2 , respectively, with $p \leq 0.05$. There were no genes that did not reach the cycle threshold value within 40 cycles.

Table S3. Changes in expression of all genes related to inflammatory response and autoimmunity in jetPEI™ or polyplex-exposed HeLa S3 cells.

GeneBank	Symbol	Description ^a	Fold Change in Gene Expression ^b					
			jetPEI™		GFP (CMV) polyplexes		GFP (EF1 α) polyplexes	
			4h	24h	4h	24h	4h	24h
NM_001706	BCL6	B-cell CLL/lymphoma 6	3.9	1.5	4.4	2.1	4.5	2.3
NM_000064	C3	Complement component 3	1.1	1.0	1.1	1.4	-1.3	-1.1
NM_004054	C3AR1	Complement component 3a receptor 1	1.6	-1.9	-1.3	18.9	2.3	19.0
NM_007293	C4A	Complement component 4A (Rodgers blood group)	-1.0	2.2	-1.6	4.8	-1.3	2.8
NM_006274	CCL19	Chemokine (C-C motif) ligand 19	1.2	-2.1	-1.2	-1.1	-1.2	-1.2
NM_002982	CCL2	Chemokine (C-C motif) ligand 2	1.5	1.5	2.6	-6.1	1.8	-1.1
NM_002989	CCL21	Chemokine (C-C motif) ligand 21	1.7	1.1	1.4	1.1	1.0	1.0
NM_002990	CCL22	Chemokine (C-C motif) ligand 22	3.6	6.8	5.4	272.8	4.3	213.1
NM_002991	CCL24	Chemokine (C-C motif) ligand 24	1.6	-1.0	-1.2	1.4	1.4	1.3
NM_002983	CCL3	Chemokine (C-C motif) ligand 3	-1.2	46.5	-1.1	1084.1	1.9	989.4
NM_002985	CCL5	Chemokine (C-C motif) ligand 5	1.1	2.4	4.5	109.6	4.1	116.2
NM_001295	CCR1	Chemokine (C-C motif) receptor 1	1.4	1.1	1.8	24.2	-2.0	20.1
NM_005508	CCR4	Chemokine (C-C motif) receptor 4	1.5	3.2	1.6	5.8	2.1	2.7
NM_001838	CCR7	Chemokine (C-C motif) receptor 7	1.9	-2.3	2.1	3.1	2.2	3.5
NM_005194	CEBPB	CCAAT/enhancer binding protein (C/EBP), beta	1.6	1.1	2.5	1.7	2.2	1.0
NM_000757	CSF1	Colony stimulating factor 1 (macrophage)	-1.1	2.1	-1.0	8.0	-1.2	6.6
NM_001511	CXCL1	Chemokine (C-X-C motif) ligand 1 (melanoma growth stimulating activity, alpha)	2.3	-1.0	1.0	-1.3	1.1	-1.7
NM_001565	CXCL10	Chemokine (C-X-C motif) ligand 10	-2.4	2.6	2.3	553.0	2.1	652.0
NM_002089	CXCL2	Chemokine (C-X-C motif) ligand 2	2.8	1.2	1.2	-1.3	1.3	-1.3
NM_002090	CXCL3	Chemokine (C-X-C motif) ligand 3	4.4	1.2	1.4	-1.8	1.8	-1.5
NM_002994	CXCL5	Chemokine (C-X-C motif) ligand 5	2.9	-2.8	3.2	-1.1	-1.1	1.1
NM_002993	CXCL6	Chemokine (C-X-C motif) ligand 6 (granulocyte chemotactic protein 2)	-2.8	9.0	6.0	-1.0	-1.8	1.5
NM_003467	CXCR4	Chemokine (C-X-C motif) receptor 4	2.3	1.3	1.6	-1.6	1.6	-1.9
NM_000639	FASLG	Fas ligand (TNF superfamily, member 6)	1.1	-1.0	1.1	1.9	1.2	-2.1
NM_001459	FLT3LG	Fms-related tyrosine kinase 3 ligand	-1.4	1.0	-1.8	2.1	-1.6	1.5
NM_005252	FOS	V-fos FBJ murine osteosarcoma viral oncogene homolog	5.3	-2.5	3.8	-2.5	3.5	-3.4
NM_006037	HDAC4	Histone deacetylase 4	-1.9	1.0	-1.6	-1.5	-1.7	-1.9
NM_000572	IL10	Interleukin 10	-1.5	1.1	-1.0	1.3	5.1	7.6
NM_000628	IL10RB	Interleukin 10 receptor, beta	-1.7	1.1	-1.5	2.1	-1.7	1.7
NM_001562	IL18	Interleukin 18 (interferon-gamma-inducing factor)	1.1	1.1	1.2	1.5	1.2	1.6
NM_000575	IL1A	Interleukin 1, alpha	-2.1	3.3	-1.0	9.0	1.1	7.3
NM_000576	IL1B	Interleukin 1, beta	-1.7	2.6	-1.2	7.3	-1.3	6.3
NM_000877	IL1R1	Interleukin 1 receptor, type I	-6.8	1.0	-3.4	3.6	-5.8	3.1
NM_002182	IL1RAP	Interleukin 1 receptor accessory protein	1.1	1.1	1.2	-1.1	1.1	-1.4
NM_000577	IL1RN	Interleukin 1 receptor antagonist	1.4	2.0	-1.1	4.6	1.0	6.0
NM_016584	IL23A	Interleukin 23, alpha subunit p19	-1.2	1.1	1.2	7.2	-1.6	6.1
NM_000600	IL6	Interleukin 6 (interferon, beta 2)	1.4	1.6	7.5	11.8	7.1	12.4
NM_000565	IL6R	Interleukin 6 receptor	1.8	2.4	1.2	1.2	1.1	-1.1
NM_000584	IL8	Interleukin 8	2.8	2.6	1.0	3.4	1.3	2.8
NM_000211	ITGB2	Integrin, beta 2 (complement component 3 receptor 3 and 4 subunit)	1.3	1.1	-1.1	1.6	1.0	1.6
NM_000595	LTA	Lymphotoxin alpha (TNF superfamily, member 1)	6.2	4.2	11.4	53.8	8.1	60.7
NM_002341	LTB	Lymphotoxin beta (TNF superfamily, member 3)	1.8	1.6	1.3	2.8	1.6	4.1
NM_015364	LY96	Lymphocyte antigen 96	-2.1	2.9	-2.4	2.5	-3.5	4.3
NM_002468	MYD88	Myeloid differentiation primary response gene (88)	-1.3	1.3	-1.3	6.0	-1.4	4.3
NM_004555	NFATC3	Nuclear factor of activated T-cells, cytoplasmic, calcineurin-dependent 3	-1.5	-1.1	-1.6	-1.0	-1.6	-1.1
NM_003998	NFKB1	Nuclear factor of kappa light polypeptide gene enhancer in B-cells 1	1.0	1.1	-1.1	1.0	-1.2	1.1
NM_000625	NOS2	Nitric oxide synthase 2, inducible	2.8	1.1	8.2	4.0	7.2	3.5
NM_000176	NR3C1	Nuclear receptor subfamily 3, group C, member 1 (glucocorticoid receptor)	-1.2	1.1	-1.1	1.9	-1.1	1.6

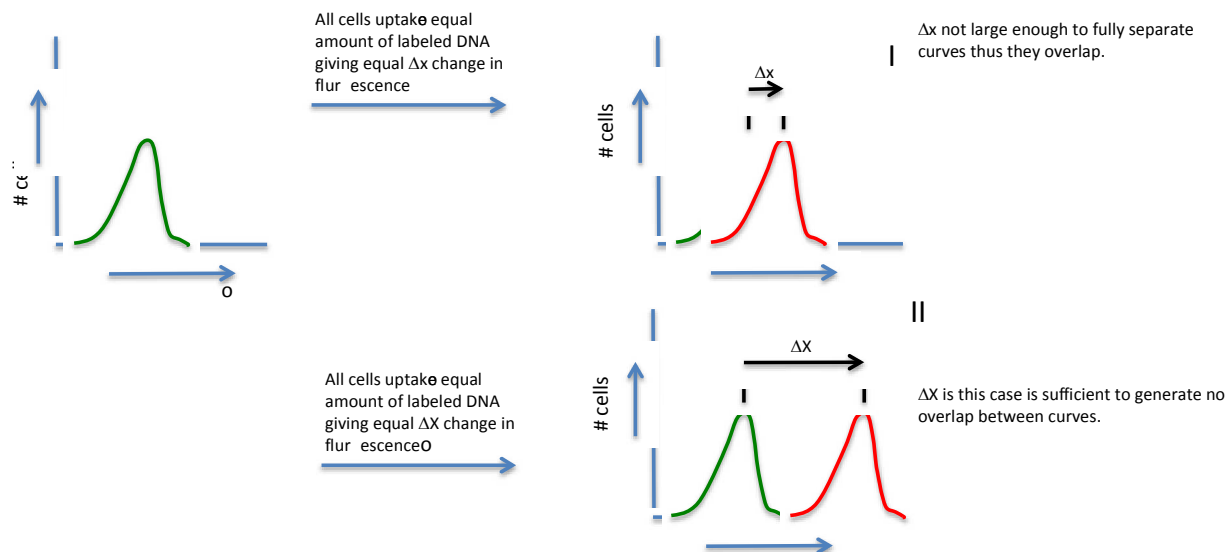
NM_003821	RIPK2	Receptor-interacting serine-threonine kinase 2	-1.4	1.2	-1.1	2.1	-1.1	2.2
NM_001039661	TIRAP	Toll-interleukin 1 receptor (TIR) domain containing adaptor protein	-3.8	-1.0	-2.4	-1.1	-3.4	-1.5
NM_003263	TLR1	Toll-like receptor 1	-5.8	1.2	-1.6	3.4	-2.4	2.8
NM_003265	TLR3	Toll-like receptor 3	-2.2	1.1	-1.9	11.5	-1.7	10.8
NM_138554	TLR4	Toll-like receptor 4	1.1	1.6	-1.2	3.9	-1.3	4.3
NM_003268	TLR5	Toll-like receptor 5	1.2	-6.5	1.5	5.8	1.5	9.6
NM_006068	TLR6	Toll-like receptor 6	-3.0	1.1	-2.2	-1.1	-2.1	-1.3
NM_016562	TLR7	Toll-like receptor 7	5.6	-1.0	3.9	-1.0	7.4	1.3
NM_000594	TNF	Tumor necrosis factor (TNF superfamily, member 2)	13.0	1.2	18.6	14.9	14.6	14.1
NM_003807	TNFSF14	Tumor necrosis factor (ligand) superfamily, member 14	1.4	2.6	4.1	5.2	3.8	2.8
NM_019009	TOLLIP	Toll interacting protein	-1.4	1.2	-1.3	1.4	-1.7	1.2

^aThe gene descriptions are reproduced from the array product information from Qiagen. ^bGreen and red shading indicate fold-changes of ≥ 2 and ≤ 2 , respectively, with $p \leq 0.05$. Genes that were analyzed on the array but that did not reach the cycle threshold value within 40 cycles are *CCL11*, *CCL13*, *CCL16*, *CCL17*, *CCL23*, *CCL4*, *CCL7*, *CCL8*, *CCR2*, *CCR3*, *CD40*, *CD40LG*, *CRP*, *CXCL9*, *IFNG*, *IL18RAP*, *IL1F10*, *IL22*, *IL22RA2*, *IL23R*, *IL8RA*, *IL8RB*, *IL9*, *KNG1*, and *TLR2*.

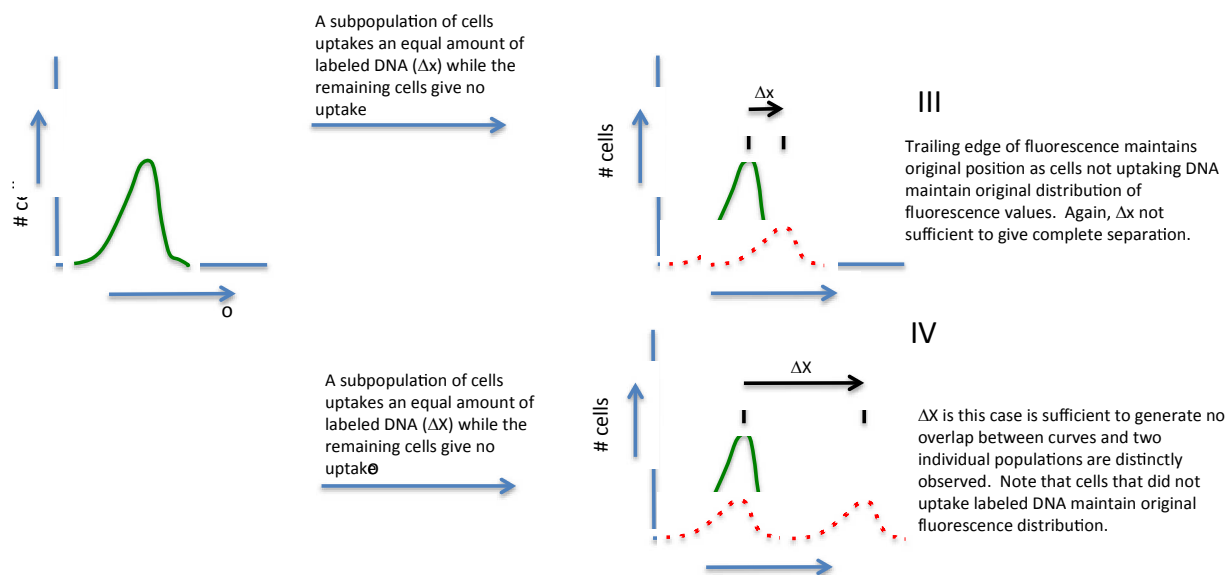
Discussion S1. Interpretation of flow cytometry for transfection (uptake) of polyplexes into HeLa S3 and 293A cells.

For this study, it is important to quantify the fraction of the cell population that has been transfected. In order to determine the percentage of cells that have taken up polyplexes, we employed polyplexes formed between jetPEITM and CX-rhodamine-labeled blank pDNA. The experimental details are provided above in the “pDNA Uptake Assay” and Figure S3. When interpreting the data in Figure S3, two aspects are important to keep in mind: 1) the total fluorescence shift is less than one order of magnitude and 2) the final fluorescence distributions of the control cells and the transfected cells overlap.

In the data presented in Figure S3, the entire population of HeLa S3 and 293A cells exhibit a mean fluorescence shift of 4500 ± 240 and 6200 ± 390 , respectively. In other words, all parts of the original fluorescence distribution of cells shift, indicating that all cells in the population have taken up the CX-rhodamine-labeled blank pDNA. This similar level of polyplex uptake across the population, at least at the level of detection of flow cytometry, is why we have treated the cells as a single transfected population for the analyses present in this paper. This general approach to treating the data is illustrated in the following schematic for two general cases of homogeneous uptake of material (cases I and II) and two general cases of inhomogeneous uptake of material (cases III and IV). The data in Figure S3 is best described by case I.



Both of cases I and II show *homogeneous* uptake of labeled DNA by the cell population, the only thing that differs is the magnitude of the fluorescence shift.



Both of cases III and IV show *inhomogeneous* uptake of labeled DNA by the cell population, the only thing that differs is the magnitude of the fluorescence shift.

We find it important to note that there is an alternative approach commonly used to interpret flow cytometry data that is inappropriate for the data shown in Figure S3. Rather than considering how the entire fluorescence distribution shifts, as we have described above, this second approach sets a cutoff defined by the fluorescence distribution of the control cells. Then,

for the transfected cells, uptake is deemed to have occurred for all cells above this cutoff level and is deemed to have not occurred for all cells below this cutoff limit.

The two approaches outlined here result in very different interpretations regarding the fraction of the cell population transfected by polyplexes in Figure S3. In the first case, the entire distribution is observed to shift in fluorescence and this fluorescence increase is ascribed to CX-rhodamine-labeled blank pDNA uptake. Therefore, roughly 100% of the cells are assigned as transfected. In the second case, $54 \pm 3\%$ of transfected HeLa S3 have crossed the cutoff level set by the control cells, so 54% of cells are assigned as transfected. (This figure is $68 \pm 1\%$ for the 293A cells.) Since this second method of interpreting flow cytometry data is commonly used (although often for expression experiments that give fluorescence shifts of many orders of magnitude, mostly similar to cases II and IV above), we found it necessary to adopt another approach to determine which interpretation method was providing the correct interpretation of transfection level for this data set.

In order to distinguish between these two different approaches to interpreting the flow cytometry data, we performed a new experiment in which both flow cytometry and confocal fluorescence microscopy were employed. Confocal fluorescence microscopy allows us to see a field of cells and directly count the fraction transfected. By counting multiple fields of cells, we can assess a fraction of uptake and compare this to the uptake values obtained by the two methods of interpreting the flow cytometry data.

For this control experiment, we again employed jetPEITM and CX-rhodamine-labeled blank pDNA to form the polyplexes. Some modifications were made to the protocol used to generate Figure S3 in order to accommodate the inclusion of confocal fluorescence microscopy in the experiment.

pDNA Uptake Measured by Confocal Microscopy and Flow Cytometry

Cells were taken through the PKH26 procedure with no PKH26 present. The cells were plated at 84,210 cells/well in 2-well coverglass chambers for confocal microscopy with 800 μ L complete medium, and incubated for 5 to 6 h at 37 °C with 5% CO₂ for 5 hours. (The number of cells was scaled up in comparison to the 80,000 used in 12-well plates to maintain consistency in the number of cells per area for growth.) Cells were transfected for 3 h as described with polyplexes formed between jetPEITM and CX-rhodamine-labeled blank pDNA according to the

manufacturer's protocol and incubated for 9 h in complete medium. Two replicates were used for each condition.

CX-rhodamine-labeled blank pDNA uptake was first assessed using confocal and differential interference contrast (DIC) microscopy. Confocal and DIC microscopy were performed on live cells in complete medium using a Leica SP5X inverted microscope system (Leica Microsystems GmbH; Wetzlar, Germany). DIC was performed at 405 nm. CX-rhodamine was excited at 575 nm (1.5 MW) and emission was measured between 595-800 nm.

Immediately following the microscopy measurements, the same cell samples were harvested and CX-rhodamine uptake was measured using flow cytometry. The cells were washed with DPBS, harvested with trypsin, and suspended in 400 μ L of DPBS. CX-rhodamine fluorescence was assessed using a BD Accuri C6 Flow Cytometer[®] by exciting at 488 nm and measuring all emission greater than 670 nm.

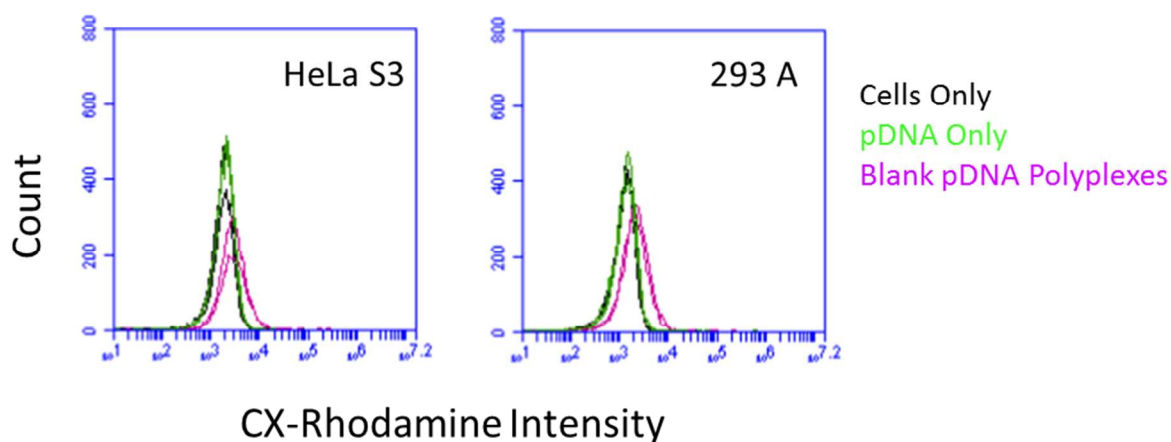


Figure S8. CX-rhodamine fluorescence intensity for representative HeLa S3 and 293A cells treated with polyplexes formed between jetPEI[™] and CX-rhodamine-labeled blank pDNA. Cells were transfected for 3 h and incubated 9 h further before being harvested and analyzed. For HeLa S3 and 293A cells the entire population of cells exhibits a mean fluorescence shift of 1443 (range of 1438 to 1448) and 1101 (1074 to 1127), respectively, consistent with a substantial degree of transfection for all cells in the population.

Once again, the entire fluorescence distribution is observed to shift with respect to the control cells (analogous to case I in the above schematic). Using the first approach to analyzing the data, we conclude that all cells have uptaken some polyplexes thus resulting in a fluorescence shift for the entire population. In other words, roughly 100% of cells have been transfected. In using the second approach to analyze the data, a cutoff is set based on the control cell population

and we conclude that roughly 20% of the cell populations has been transfected. Clearly, the two approaches to data interpretation give substantially different answers. Can this be resolved by confocal fluorescence microscopy?

For the confocal fluorescence microscopy analysis, fluorescent cells were counted in multiple fields for both 293A and HeLa S3 cells. The results are summarized in the following table with data given in each column for the total number of microscopy fields of view employed, the total number of fluorescent cells observed/total cells observed, and the percentage this represents.

Cell Type	Cells only control	CX-rhodamine-labeled DNA only exposed cells	Polyplex-Exposed Cells
HeLa S3	6, 0/632, 0%	6, 4/566, 0.7%	9, 422/484, 87%
293A	3, 0/283, 0%	6, 7/763, 0.1%	8, 751/793, 95%

In this case, the confocal data clearly supports the first approach to interpreting the flow cytometry data, and is in good agreement with the conclusion that almost all cells incorporate polyplexes, thereby exhibiting a fluorescence shift. The second method of interpreting the flow cytometry data, resulting in an estimate of roughly 20% uptake, is clearly inconsistent with the confocal microscopy analysis *of the same population of cells*. Examples of the confocal micrographs are provided below. We note that there is a difference in pDNA uptake between the data in Figure S3 (~50% to 70%) and that in Figure S8 (~20%) when measured according to the flow cytometry cutoff method. The uptake is likely lower in Figure S8 because of the additional hours that microscopy measurements added between the end of incubation and the actual flow cytometry measurements.

We conclude this supplemental discussion of the determination of the fraction of cells transfected by the polyplexes with two major conclusions. First, both flow cytometry and confocal fluorescence microscopy provide clear and conclusive evidence that ~90-100% of the 293A and HeLa S3 cells are transfected by the polyplexes under the conditions reported herein. Second, we note that the method of setting flow cytometry cutoffs to make population assessments is appropriate for data illustrated by cases II and IV in the above schematic, but is inappropriate for data illustrated by cases I and III. The data for the transfection study in this

paper is the same as case I; therefore the second method is inappropriate for interpreting the data shown in Figure S3.

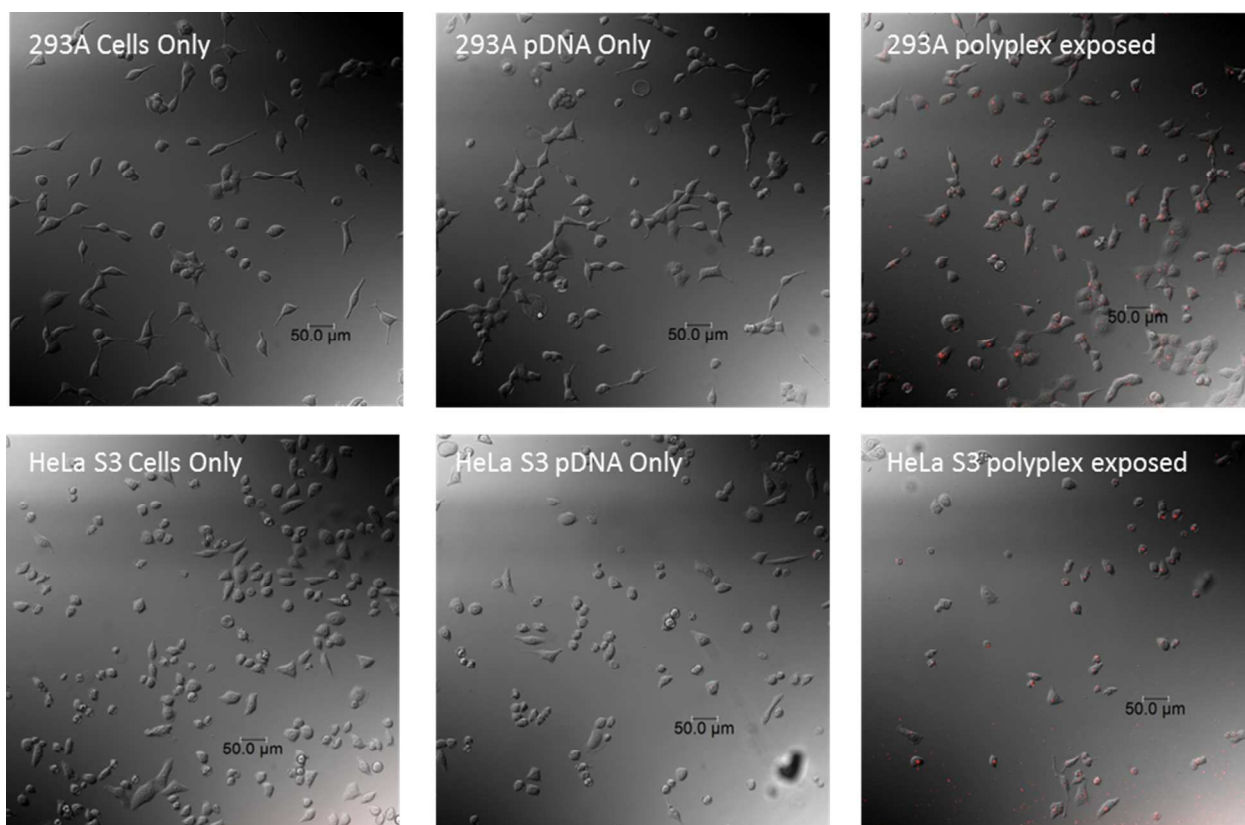


Figure S9. Images obtained using confocal and DIC microscopy show that 87% and 95% of HeLa S3 and 293A cells, respectively, exposed to polyplexes formed between CX-rhodamine-labeled blank pDNA and jetPEITM are positive for CX-rhodamine.